

First description of revertant mosaicism in familial platelet disorder with predisposition to acute myelogenous leukemia: correlation with the clinical phenotype

Ana C. Glembotsky,^{1,2*} Cecilia P. Marin Oyarzún,^{1,2,3*} Geraldine De Luca,^{1,2} Christophe Marzac,^{3,4} Nathalie Auger,⁵ Nora P. Goette,⁴ Rosana F. Marta,^{1,2} Hana Raslova^{3#} and Paula G. Heller^{1,2#}

¹Instituto de Investigaciones Médicas A. Lanari, Facultad de Medicina, Universidad de Buenos Aires, Buenos Aires, Argentina; ²Departamento Hematología Investigación, Consejo Nacional de Investigaciones Científicas y Técnicas (CONICET), Universidad de Buenos Aires, Instituto de Investigaciones Médicas (IDIM), Buenos Aires, Argentina; ³INSERM UMR 1170, Gustave Roussy Cancer Campus, Université Paris-Saclay, Equipe Labellisée par la Ligue Nationale Contre le Cancer, Villejuif, France; ⁴Department of Medical Biology and Pathology, Gustave Roussy Cancer Campus, Université Paris-Saclay, Villejuif, France and ⁵Department of Tumor Genetics, Gustave Roussy Cancer Campus, Université Paris-Saclay, Villejuif, France

*ACG and CPMO contributed equally as co-first authors.

#HR and PGH contributed equally as co-senior authors.

Correspondence: PAULA G. HELLER - paulaheller@hotmail.com

doi:10.3324/haematol.2020.253070

Supplementary Methods

Biological samples

Samples were obtained from the proband and family members who presented with platelet defects without or prior to malignant transformation. DNA was obtained from whole blood, oral swabs and purified blood cell populations. Briefly, mononuclear cells were isolated using a Ficoll-Hypaque gradient followed by magnetic cell separation of B and T cells using CD19 and CD3 microbeads (Miltenyi Biotec, Germany), respectively. Granulocytes were recovered from the bottom layer and subjected to dextran sedimentation and red cell hypotonic lysis. Hematopoietic progenitors (CD34⁺) were isolated from mononuclear cells by immunomagnetic enrichment (Miltenyi, Biotec), stained with CD34-PE antibody (Beckton Dickinson) and sorted by the Influx flow cytometer (Beckton Dickinson). They were cultured in serum-free medium in the presence of a cocktail of human recombinant cytokines containing EPO (1 U/mL) (Amgen Thousand Oaks, CA), TPO (20 ng/mL) (Kirin, Japan), SCF (25 ng/mL) (Biovitrum AB, Sweden), IL-3 (10 ng/mL) (MiltenyiBiotec), FLT3-L (10 ng/mL), G-CSF (20 ng/mL) and IL-6 (100 U/mL) for 8 days, pelleted and stored at -80°C. DNA was extracted using standard procedures. DNA concentrations and OD260/280 ratio were measured with the NanoDrop 1000 spectrophotometer (Thermo Fisher Scientific Inc., Waltham, MA) and DNA integrity was assessed by electrophoresis.

To obtain platelet RNA, platelet-rich plasma (PRP) was prepared by centrifugation at 200g for 10 min at room temperature, supplemented with 0.042M indomethacin, subjected to an additional centrifugation step at 200 g during 8 min to remove leukocytes and red cells, filtered through a leukocyte reduction filter (Purecell PL, Pall Biomedical Products Co, NY, USA) and red blood cells were lysed with 8.6 g/L ammonium chloride solution. After this procedure, the leukocyte:platelet ratio was <1:10⁶. Total RNA was prepared from 1-3x10⁹ platelets using glycogen as a carrier and 1 µg RNA was reverse transcribed using SuperScript (Life Technologies, Carlsbad, CA, USA).

Sanger sequencing

Amplification of a fragment of the *RUNX1* gene spanning the previously characterized familial mutation (exon 7) and a region of *ATM* encompassing the mutation found by NGS (exon 58) was done by PCR. To exclude allelic drop-out yielding random non-amplification of *RUNX1* mutant allele, a previously sequenced DNA fragment bearing no polymorphisms was sequenced using a different pair of primers, as detailed below. The amplified fragments were purified using the ADN PuriPrep GP kit (Inbio Highway, Argentina), followed by Sanger bidirectional sequencing using

the respective forward (F) or reverse (R) primer for fluorescent labelling and analysis on an ABI 3100/3730XL or ABI PRISM 310 Analyzer (Applied Biosystems, Foster City, CA, USA).

Next generation sequencing (NGS)

2 methods were used:

1) The mutated *RUNX1* region was amplified by PCR using primers listed below. PCR products were end-repaired, extended with an 'A' base on the 3'end, ligated with indexed paired-end adaptors (NEXTflex, Bioo Scientific) using the Bravo Platform (Agilent) and amplified by PCR for 4 cycles. Amplicon libraries were sequenced in an IlluminaMiSeq flow cell using the onboard cluster method, as paired-end sequencing (2x250 bp reads) (Illumina, San Diego, CA).

	Forward	Reverse
RUNX1 DNA 1	GGCATATCTCTAGCGAGTCTATGTT	CAGAGCTCCTCGTATCCTCTGTA
RUNX1 DNA 2	AAAGGGGGCCATTCTGCT	CCTTGTGGGGATCTGGTTAC
RUNX1 DNA 3	CTGATCTCTCCCTCCCTCC	AGGTGGTGCTGTTGGTTCG
RUNX1 DNA 4*	CTGATCTCTCCCTCCCTCC	ATCTGACTCTGAGGCTGAG
RUNX1 cDNA*	GAAGACATCGGCAGAACTA	GAGGCAATGGATCCCAGGTA
ATM	GAAGTCTTCATGGATGTTTGCC	GCCAAACAACAAAGTGCTCA

Primer sequences used for Sanger sequencing and targeted NGS.

* primers used for targeted NGS

2) NGS gene panel

A panel of 77 genes designed for the diagnosis of myeloid malignancies used for NGS includes: *ABL1* (Chr9; NM_007313 ;exons 4-9), *ADGRV1*(chr5 ; NM_032119 ; exons 1-90), *ANKRD26* (Chr10 ; NM_014915 ; exon 1 and 5'UTR), *APC* (Chr5 ; NM_001127510; exons 1-15), *ASXL1* (Chr20;NM_015338; exons 11-12), *ASXL2* (Chr2; NM_018263; exons 11-12), *ATG2B* (Chr14 ; 20 polymorphisms), *ATM* (Chr11; NM_000051; exons 2-63), *ATRX* (ChrX ; NM_000489 ; exons 1-35), *BCOR* (ChrX; NM_001123385; exons 3-16), *BCORL1* (ChrX ; NM_001184772 ; exons 1-13), *BRAF* (Chr7 ; NM_004333 ; exon 15), *CALR* (Chr19; NM_004343; exon 9), *CBL* (Chr11; NM_005188; exons 4, 8-9,12,16), *CEBPA* (Chr19; NM_001287424; exon 1), *CHEK2* (Chr22 ; NM_001005735 ; exons 3-16), *CREBBP* (Chr16 ; NM_004380 ; exons 1-31), *CSF3R* (Chr1; NM_156039 ; exons 14 et 17), *CUX1*(Chr7 ; NM_001202543 ; exons 1-24), *DDX41* (Chr5; NM_016222; exons 1-17), *DDX54* (chr12 ; NM_001111322 ; exons 1-20), *DHX29* (chr5 ; NM_019030 ; exons 1-27), *DIS3* (chr13 ; NM_014953 ; exons 1-21), *DNMT3A* (Chr2;

*NM_022552; exons 2-23), EED (Chr11 ; NM_001308007 ; exons 1-13), EP300 (Chr22 ; NM_001429 ; exons 1-31), EPOR (Chr19 ; NM_000121 ; exon 8), ERBB4 (Chr2 ; NM_005235 ; exons 1-28), ETNK1 (Chr12 ; NM_018638 ; exon3), ETV6 (Chr12 ; NM_001987 ; exons 1-8), EZH2 (Chr7; NM_004456; exons 2-20), FLT3 (Chr13; NM_004119; exons 8-21), GATA1 (ChrX ; NM_002049 ; exons 2-4), GATA2 (Chr3;NM_032638; exons 4-6 ; c.1017_462-703), HRAS (Chr11; NM_005343; exons 2-3 and Codon 117 in exon 4), IDH1 (Chr2; NM_005896, Codons 130-134 in exon 4), IDH2 (Chr15; NM_002168 ; exon 4), JAK2 (Chr9; NM_004972; exons 3-25 ; 46/1 Haplotype ; c.*122G>A), KDM6A (ChrX; NM_001291415 ; exons 1-30), KMT2A (Chr11;6 polymorphisms), KIT (Chr4; NM_000222; exons 2, 8-17), KRAS (Chr12; NM_033360 ; exons 2 and 4 ; Codons 57-64 in exon 3), MPL (Chr1; NM_005373; exons 1-12), MYC (Chr8; NM_002467; exon 2), NF1 (Chr17; NM_001042492; exons 1-58), NFE2 (chr12 ; NM_001261461 ; exons 3-4), NPM1 (chr5; NM_002520; exon 11), NRAS (Chr1; NM_002524; exons 2-3), PHF6 (ChrX; NM_001015877; exons 2-10), PPM1D (Chr17 ; NM_003620 ; exon 6), PRPF40B (Chr12 ; NM_001031698 ; exons 1-26), PRPF8 (Chr17 ; NM_006445 ; exons 2-43), PTPN11 (Chr12;NM_002834; exons 3-4;8;11-13), RAD21 (Chr8; NM_006265; exons 2-14), RUNX1 (Chr21; NM_001001890; exons 3-9), SETBP1 (Chr18; NM_015559; exon 4), SETD2 (Chr3 ; NM_014159; exons 5-9), SF1 (Chr11 ; NM_004630 ; exons 1-13), SF3A1 (Chr22 ; NM_005877 ; exons 1-16), SF3B1(Chr2; NM_012433; exons 13-16), SH2B3 (chr12; NM_005475 ; exons 2-8), SIMC1 (Chr5 ; NM_001308195 ; exons 2-10), SMC1A (ChrX ; NM_6306; exons 1-25), SMC3 (Chr10;NM_5445; exons 1-29), SRP72 (Chr4 ; NM_006947 ; exons 1-19), SRSF2 (Chr17; NM_001195427 ; exon 1), STAG2 (ChrX; NM_001042749; exons 3-35), SUZ12 (Chr17 ; NM_015355 ; exons 1-16), TERC (Chr3 ; NR_001566), TERT (Chr5 ; NM_198253 ; exons 1-16), TET2 (Chr4; NM_001127208; exons 3-11), THPO (Chr3 ; NM_001289998 ; 5'UTR), TP53 (Chr17; NM_001126112 ; exons 2-11 ; NM_001126113_Exon 10; NM_001126114_Exon 10), U2AF1 (Chr21; NM_001025203; Codon 34 in exon 2 and Codon 157 in exon 6), U2AF2 (Chr19 ; NM_007279 ; exons 1-12), WT1 (Chr11; NM_024426; exons 1-4; 7-9), ZRSR2 (ChrX; NM_005089; exons 1-11).*

Libraries were obtained from 200 ng of genomic DNA using HaloPlex Target Enrichment System (Agilent technologies) and sequencing was performed using a MiSeq sequencer (Illumina, San Diego, CA), according to the manufacturer's protocols. Results were analysed after alignment of the reads using two dedicated pipelines, SOPHiA DDM[®] (Sophia Genetics) and an in-house software GRIIO-Dx[®]. For all samples, an average depth exceeding 200X for > 90% of the target regions was required. All pathogenic variants were manually checked using Integrative Genomics Viewer software. The disease-causing potential of variants was checked by using online prediction programs which included Polyphen2, MutationTaster and SIFT.

Cytoscan high density (HD) SNP array

Chromosome analysis was performed using CytoScan HD array/Oncoscan (Affymetrix) according to the manufacturer's recommendations. The data from microarray scans were extracted by Chromosome Analysis Suite software (ChAS; v3.1, Affymetrix) and analysed as previously reported.¹

Platelet features

Platelet studies were performed as previously described.^{2,3} Briefly, platelet aggregation was evaluated in PRP by light transmission aggregometry (LTA) using a lumiaggregometer (Chrono Log Corp., Havertown, PA, USA) after stimulation with 1 mM arachidonic acid, 4 µg/mL collagen, 2 µM ADP, and 1 µM epinephrine (Biopool, Bray, Ireland) and expressed as maximal light transmission percentage. To study dense (δ)-granule content, PRP was adjusted to 100×10^9 /L platelets, labelled with 2mM mepacrine (Sigma-Aldrich Inc.) for 30 minutes at room temperature, analysed by flow cytometry and a ratio between mean fluorescence intensity (MFI) with and without mepacrine was calculated and expressed as relative fluorescence intensity (RFI). To assess platelet surface expression of integrin $\alpha 2$ (GPIa) and $\beta 1$ (GPIIa) subunits of collagen receptor $\alpha 2\beta 1$, PRP was adjusted to 10×10^9 /L platelets, incubated with fluorescein isothiocyanate (FITC)-conjugated monoclonal antibody against GPIa (CD49b) and phycoerythrin (PE)-conjugated antibody against GPIIa (CD29) (BD Biosciences, San José, CA, USA) or the corresponding isotypic controls, analysed in a flow cytometer and expressed as a ratio between the antibody and the isotypic control (RFI). The platelet population was identified by labelling with CD41-PE or CD61-FITC, respectively. Assays were run in duplicate. To assess levels of other glycoproteins (GP), platelets were labelled with FITC or PE-conjugated antibodies against GPVI, GPIIb (CD41a), GPIIIa (CD61), GPIb (CD42b) and GPIX (CD42a) (BD Biosciences). For all assays, a healthy subject was studied simultaneously. Mean platelet diameter (MPD) was determined by measuring the largest diameter of 100 platelets in May–Grünwald-Giemsa-stained blood smears by using the VideoTesT-Master (Morphology) image analysis software (St Petersburg, USSR). Reference values for platelet studies were established by the mean \pm two standard deviations values of healthy subjects (n=6-20).

MYH10 expression levels in platelets by qPCR

Platelet RNA was prepared from the proband, three affected family members (II-1, III-1 and III-3) and 5 healthy subjects. Platelet *MYH10* expression was measured in triplicate by qPCR (primer sequences, forward 5'-TGCATGCTTCAAGATCGTGAG-3'; reverse 5'-AGCAACATGGGCAAGGTAAGTACTG-3') relative to *GAPDH* using SYBR® Green (Life Technologies, Grand Island, NY, USA) in an iCycler (Bio Rad Life Science, Hercules, CA, USA).

The identity of the PCR products was assessed by melting analysis and electrophoresis. Serial cDNA dilutions were assessed to ensure similar amplification efficiency of the target and control genes.

Circulating CD34⁺ cells

Whole blood was incubated with fluorescein isothiocyanate (FITC)-conjugated anti-CD45 monoclonal antibody and phycoerythrin (PE)-conjugated anti-CD34 monoclonal antibody (BD Biosciences) or the corresponding isotype control. FACS Lysing Solution (BD Biosciences) was then added to lyse the red blood cells. After washing, cells were fixed with 1% paraformaldehyde, analysed by flow cytometry and the percentage of CD34⁺ cells was calculated as described.⁴

Statistical analysis

Comparison between patients and controls was performed by Mann-Whitney test. *P* values <0.05 were considered significant.

Supplementary Tables

Table S1. Classification of the germline variant using ClinGen Myeloid Malignancy Variant Curation Expert Panel criteria for germline *RUNX1* variants

<i>RUNX1</i> variant	ClinGen classification	Rules applied
c.735delC (p.Thr246Argfs*8)	Likely Pathogenic	Absent from controls (PM2), null variant in a gene where LOF is a known mechanism of disease (PVS1_strong)*, 1 proband meeting at least one of <i>RUNX1</i> phenotypic criteria (PS4_supporting), segregation in 5 affected family members (PP1_moderate).

* PVS1_strong criteria was applied because the variant was previously shown to escape nonsense-mediated decay⁵ but the altered region is critical to protein function, as specified in Luo et al.⁶

RefSeq NM_001754 (*RUNX1* isoform c) was used.

Table S2. Hematologic features in the proband and affected family members

	CD34+ (%)	Hemoglobin (gr/dL)	WBC (x 10 ⁹ /L)	MPD (μm)	MPV (fL)	GPIIa	GPVI	GPIIb RFI (P/C)	GPIIIa RFI (P/C)	GPIb RFI (P/C)	GPIX RFI (P/C)
Proband, age 1	nd	12.2	13.1	nd	8.6	nd	nd	nd	nd	nd	nd
Proband, age 2	nd	12.7	6.5	2.3	9.3	nd	nd	nd	nd	nd	nd
Proband, age 6	nd	13.9	8.4	2.6	9.3	nd	nd	nd	nd	nd	nd
Proband, age 7	nd	13.6	6.0	2.3	8.7	nd	nd	nd	nd	nd	nd
Proband, age 10	0.02	14.7	5.3	2.4	9.0	0.78	0.80	1.01	0.84	0.86	0.91
Proband, age 12	nd	12.0	4.6	2.5	9.4	nd	nd	nd	nd	nd	nd
Affected relatives	0.05 (0.05-0.06)	13.3 (12.5-13.8)	6.5 (5.9-6.9)	3.0 (2.5-3.1)	9.9 (9.6-10.2)	0.65 (0.4-0.7)	0.80 (0.8-0.9)	0.79 (0.8-1.0)	1.02 (0.9-1.0)	1.51 (1.4-1.6)	1.74 (1.3-1.8)
Reference values	0-0.04	12-16	4-10	2.3-3.1	8.9-10.5	0.81-1.19	0.73-1.27	0.78-1.22	0.78-1.22	0.65-1.35	0.81-1.19

WBC means white blood cells, MPD; mean platelet diameter; MPV, mean platelet volume; GP, glycoprotein; RFI; relative fluorescence intensity; P/C, patient/control ratio.

GPIIa represents the β1 subunit of collagen receptor α2β1. Age of the proband is given in years. Values in affected relatives (n= 2 for circulating CD34+ cells; n=3 for platelet GPs; n=4 for all other parameters) are given as median and range. Data on platelet GPs in affected relatives was previously published.³

Normal reference values for all tested parameters are provided at the bottom of the table.

Supplementary Figures

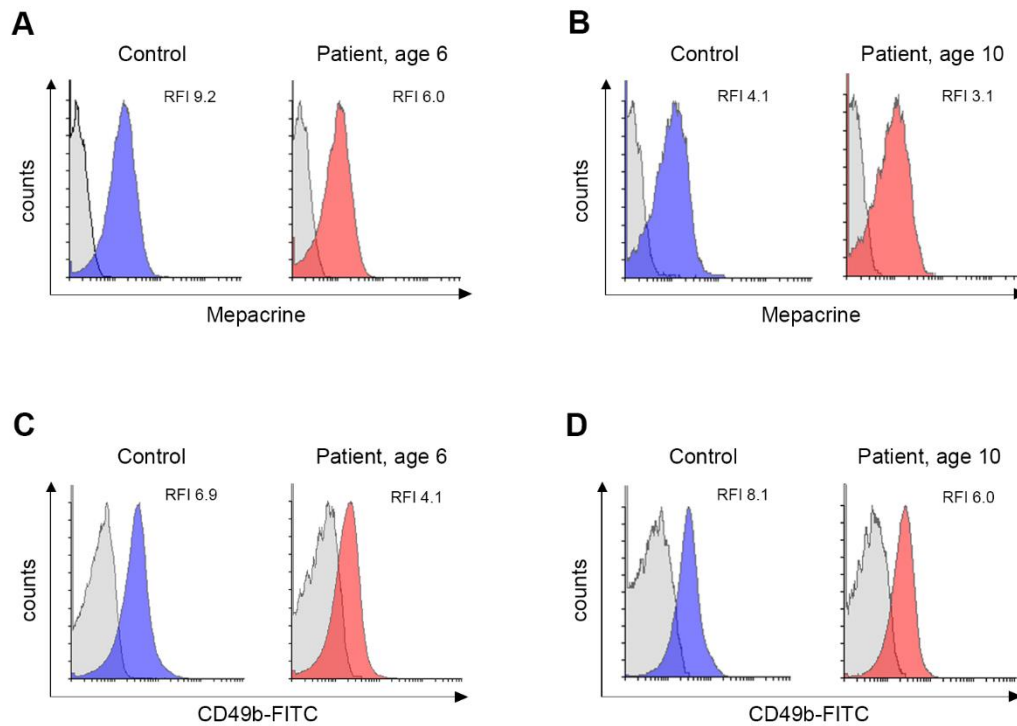


Figure S1. FPD/AML-related platelet features. Dense granule content in the proband (A) at the age of 6 years and (B) at the age of 10 years. Platelets were incubated with mepacrine, analysed by flow cytometry and a ratio between mean fluorescence intensity of platelets incubated with and without mepacrine was calculated and expressed as relative fluorescence intensity (RFI). A control sample was run simultaneously with the patient at both time points. Colour histograms represent platelets incubated with mepacrine and gray histograms, those without mepacrine. Surface expression of GPIa (C) at the age of 6 years and (D) at the age of 10 years. Platelets were incubated with FITC-conjugated CD49b or the corresponding isotype control, analysed by flow cytometry and a ratio between mean fluorescence intensity of CD49b and the isotype control was expressed as relative fluorescence intensity (RFI). A control sample was run simultaneously with the patient at both time points. Colour histograms represent platelets stained with CD49b and gray histograms, isotype controls.

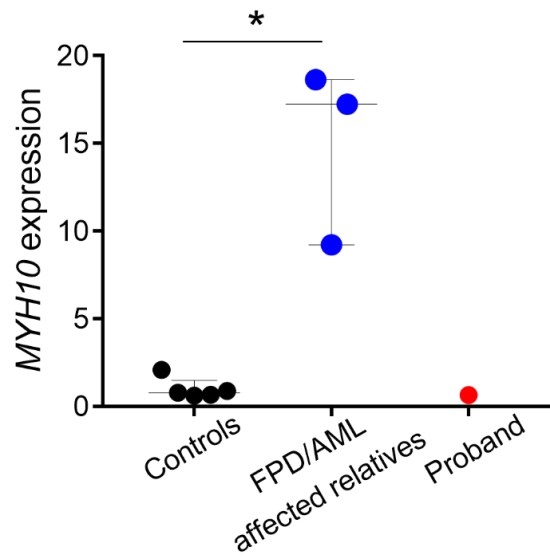


Figure S2. *MYH10* gene expression in platelets. Real-time PCR analysis of *MYH10* (myosin 10) relative to *GAPDH* in platelets from the proband, affected family members (n=3) and healthy subjects (n=5). * $P < 0.05$, Mann-Whitney test.

Supplementary References

1. Popova T, Manié E, Stoppa-Lyonnet D, Rigai G, Barillot E, Stern MH. Genome Alteration Print (GAP): a tool to visualize and mine complex cancer genomic profiles obtained by SNP arrays. *Genome Biol.* 2009;10(11):R128.
2. Glembotsky AC, Bluteau D, Espasandin YR, et al. Mechanisms underlying platelet function defect in a pedigree with familial platelet disorder with a predisposition to acute myelogenous leukemia: potential role for candidate *RUNX1* targets. *J Thromb Haemost.* 2014;12(5):761-772.
3. Glembotsky AC, Sliwa D, Bluteau D, et al. Downregulation of TREM-like transcript (TLT)-1 and collagen receptor $\alpha 2$ subunit, two novel *RUNX1*-targets, contributes to platelet dysfunction in familial platelet disorder with predisposition to acute myelogenous leukemia. *Haematologica.* 2019; 104 (6): 1244-1255.
4. Keeney M, Chin-Yee I, Weir K, Popma J, Nayar R, Sutherland DR. Single platform flow cytometric absolute CD34+ cell counts based on the ISHAGE guidelines. *International Society of Hematotherapy and Graft Engineering. Cytometry.* 1998;34(2):61-70.
5. Heller PG, Glembotsky AC, Gandhi MJ, et al. Low Mpl receptor expression in a pedigree with familial platelet disorder with predisposition to acute myelogenous leukemia and a novel *AML1* mutation. *Blood.* 2005;105(12):4664-4670.
6. Luo X, Feurstein S, Mohan S, et al. ClinGen Myeloid Malignancy Variant Curation Expert Panel recommendations for germline *RUNX1* variants. *Blood Adv.* 2019; 3(20): 2962–2979.

7. Yoshimi A, Toya T, Kawazu M, et al. Recurrent CDC25C mutations drive malignant transformation in FPD/AML. *Nat Commun.* 2014;5(1):4770.
8. Kanagal-Shamanna R, Loghavi S, DiNardo CD, et al. Bone marrow pathologic abnormalities in familial platelet disorder with propensity for myeloid malignancy and germline RUNX1 mutation. *Haematologica.* 2017;102(10):1661-1670.
9. Johnson B, Lowe GC, Futterer J, et al; UK GAPP Study Group. Whole exome sequencing identifies genetic variants in inherited thrombocytopenia with secondary qualitative function defects. *Haematologica.* 2016;101(10):1170-1179.
10. Pastor V, Hirabayashi S, Karow A, et al. Mutational landscape in children with myelodysplastic syndromes is distinct from adults: specific somatic drivers and novel germline variants. *Leukemia.* 2017;31(3):759-762.
11. De Rocco D, Melazzini F, Marconi C, et al. Mutations of RUNX1 in families with inherited thrombocytopenia. *Am J Hematol.* 2017;92(6):E86-E88.
12. Ouchi-Uchiyama M, Sasahara Y, Kikuchi A, et al. Analyses of genetic and clinical parameters for screening patients with inherited thrombocytopenia with small or normal-sized platelets. *Pediatr Blood Cancer.* 2015;62(12):2082-2088.
13. Guidugli L, Johnson AK, Alkorta-Aranburu G, et al. Clinical utility of gene panel-based testing for hereditary myelodysplastic syndrome/acute leukemia predisposition syndromes. *Leukemia.* 2017;31(5):1226-1229.
14. Marneth AE, van Heerde WL, Hebeda KM, et al. Platelet CD34 expression and α/δ -granule abnormalities in GFI1B- and RUNX1-related familial bleeding disorders. *Blood.* 2017;129(12):1733-1736.
15. Di Nardo CD, Bannan SA, Routbort M, et al. Evaluation of patients and families with concern for predispositions to hematologic malignancies within the Hereditary Hematologic Malignancy Clinic (HHMC). *Clin Lymphoma Myeloma Leuk.* 2016;16(7):417-428.e2.
16. Chin DWL, Sakurai M, Nah GSS, et al. RUNX1 haploinsufficiency results in granulocyte colony-stimulating factor hypersensitivity. *Blood Cancer J.* 2016; 6(1):e379.
17. Ng IKS, Lee J, Ng C, et al. Preleukemic and second-hit mutational events in an acute myeloid leukemia patient with a novel germline RUNX1 mutation. *Biomark Res.* 2018;6(1):16.
18. Zhang MY, Keel SB, Walsh T, et al. Genomic analysis of bone marrow failure and myelodysplastic syndromes reveals phenotypic and diagnostic complexity. *Haematologica.* 2015;100(1):42-48.
19. Chisholm KM, Denton C, Keel S, et al. Bone marrow morphology associated with germline RUNX1 mutations in patients with familial platelet disorder with associated myeloid malignancy. *Pediatr Dev Pathol.* 2019;22(4):315-328.

20. Badin MS, Iyer JK, Chong M, et al. Molecular phenotype and bleeding risks of an inherited platelet disorder in a family with a RUNX1 frameshift mutation. *Haemophilia*. 2017;23(3):e204-e213.
21. Langabeer SE, Owen CJ, McCarron SL, et al. A novel RUNX1 mutation in a kindred with familial platelet disorder with propensity to acute myeloid leukaemia: male predominance of affected individuals. *Eur J Haematol*. 2010;85(6):552-553.
22. Tawana K, Wang J, Király PA, et al. Recurrent somatic JAK-STAT pathway variants within a RUNX1-mutated pedigree. *Eur J Hum Genet*. 2017;25(8): 1020-1024.
23. Holme H, Hossain U, Kirwan M, Walne A, Vulliamy T, Dokal I. Marked genetic heterogeneity in familial myelodysplasia/acute myeloid leukaemia. *Br J Haematol*. 2012;158(2):242-248.